

Title	Stability of hexafluoroacetylacetone molecules on metallic and oxidized nickel surfaces in atomic-layer-etching processes
Author(s)	Basher, Abdulrahman H.; Krstić, Marjan; Takeuchi, Takae et al.
Citation	Journal of Vacuum Science and Technology A: Vacuum, Surfaces and Films. 38(2) p.022610
Issue Date	2020-03
oaire:version	VoR
URL	https://hdl.handle.net/11094/78313
rights	© 2020 Author(s). This article is licensed under a Creative Commons Attribution 4.0 International License.
Note	

Osaka University Knowledge Archive : OUKA

<https://ir.library.osaka-u.ac.jp/>

Osaka University

Stability of hexafluoroacetylacetone molecules on metallic and oxidized nickel surfaces in atomic-layer-etching processes

Cite as: J. Vac. Sci. Technol. A **38**, 022610 (2020); <https://doi.org/10.1116/1.5127532>

Submitted: 12 September 2019 . Accepted: 03 February 2020 . Published Online: 24 February 2020

Abdulrahman H. Basher , Marjan Krstić , Takae Takeuchi , Michiro Isobe, Tomoko Ito , Masato Kiuchi , Kazuhiro Karahashi , Wolfgang Wenzel , and Satoshi Hamaguchi 

COLLECTIONS

Paper published as part of the special topic on [Special Topic Collection on Atomic Layer Etching \(ALE\)](#)

Note: This paper is part of the 2020 Special Topic Collection on Atomic Layer Etching (ALE).



View Online



Export Citation



CrossMark

ARTICLES YOU MAY BE INTERESTED IN

[Thermal atomic layer etching of metallic tungsten via oxidation and etch reaction mechanism using O₂ or O₃ for oxidation and WCl₆ as the chlorinating etchant](#)

Journal of Vacuum Science & Technology A **38**, 022605 (2020); <https://doi.org/10.1116/1.5134430>

[Thermal atomic layer etching of silicon nitride using an oxidation and “conversion etch” mechanism](#)

Journal of Vacuum Science & Technology A **38**, 022607 (2020); <https://doi.org/10.1116/1.5140481>

[Thermal etching of AlF₃ and thermal atomic layer etching of Al₂O₃](#)

Journal of Vacuum Science & Technology A **38**, 022603 (2020); <https://doi.org/10.1116/1.5135911>



Instruments for Advanced Science

Contact Hiden Analytical for further details:
W www.HidenAnalytical.com
E info@hiden.co.uk

CLICK TO VIEW our product catalogue

Gas Analysis

- dynamic measurement of reaction gas streams
- catalysis and thermal analysis
- molecular beam studies
- dissolved species probes
- fermentation, environmental and ecological studies

Surface Science

- UHV TPD
- SIMS
- end point detection in ion beam etch
- elemental imaging - surface mapping

Plasma Diagnostics

- plasma source characterization
- etch and deposition process reaction kinetic studies
- analysis of neutral and radical species

Vacuum Analysis

- partial pressure measurement and control of process gases
- reactive sputter process control
- vacuum diagnostics
- vacuum coating process monitoring

Stability of hexafluoroacetylacetone molecules on metallic and oxidized nickel surfaces in atomic-layer-etching processes

Cite as: J. Vac. Sci. Technol. A 38, 022610 (2020); doi: 10.1116/1.5127532

Submitted: 12 September 2019 · Accepted: 3 February 2020 ·

Published Online: 24 February 2020



Abdulrahman H. Basher,^{1,a)} Marjan Krstić,² Takae Takeuchi,³ Michiro Isobe,¹ Tomoko Ito,¹ Masato Kiuchi,^{1,4} Kazuhiro Karahashi,¹ Wolfgang Wenzel,² and Satoshi Hamaguchi^{1,b)}

AFFILIATIONS

¹Center for Atomic and Molecular Technologies, Osaka University, 2-1 Yamadaoka, Suita, Osaka 565-0871, Japan

²3DMM2O—Cluster of Excellence (EXC-2082/1—390761711), Karlsruhe Institute of Technology (KIT), Institute of Nanotechnology, Hermann-von-Helmholtz-Platz 1, 76344 Eggenstein-Leopoldshafen, Germany

³Department of Chemistry, Faculty of Science, Nara Women's University, Kitauoya-Higashimachi, Nara 630-8506, Japan

⁴National Institute of Advanced Industrial Science & Technology, 1 Chome-8-31 Midorigaoka, Ikeda, Osaka 563-8577, Japan

Note: This paper is part of the 2020 Special Topic Collection on Atomic Layer Etching (ALE).

^{a)}Electronic mail: a.h.basher@ppl.eng.osaka-u.ac.jp

^{b)}Electronic mail: hamaguch@ppl.eng.osaka-u.ac.jp

ABSTRACT

Adsorption of enol hexafluoroacetylacetone (hfacH) on nickel oxide (NiO) fcc (100) and metallic Ni fcc (100) surfaces and the stability of the adsorbate was examined using first-principles quantum mechanical simulations. It was shown that an hfacH molecule can be unstable and dissociate on an Ni metal surface. On an NiO surface; however, an hfacH molecule can be deprotonated and form a hexafluoroacetylacetonate anion (hfac[−]) bonded stably with positively charged Ni atoms of the surface. The results are consistent with observations of the interaction of hfacH with NiO and Ni surfaces in earlier experiments. The results also explain the mechanisms of the adsorption steps in the thermal atomic layer etching of Ni based on the cyclic processes of surface oxidation and formation of volatile organo-nickel complexes.

© 2020 Author(s). All article content, except where otherwise noted, is licensed under a Creative Commons Attribution (CC BY) license (<http://creativecommons.org/licenses/by/4.0/>). <https://doi.org/10.1116/1.5127532>

I. INTRODUCTION

Atomic layer etching (ALE) via formation of volatile organometallic complexes is expected to establish low-damage and atomically controlled etching processes.^{1–9} Hexafluoroacetylacetone (hfacH) may be used as an etchant gas for etching various metal oxides including magnetic materials.^{1,5,6,10} When hfacH gas molecules are exposed to a metal oxide surface at room temperature, they are expected to form organometallic complexes such as Ni (hfac)₂, which is volatile at higher surface temperatures. In this process, hydrogen atoms removed from the hfacH also form volatile water molecules and remove oxygen from the surface, whereby the etching of a metal oxide proceeds thermally.^{1,2,4,7}

As an application of such a process with hfacH molecules, a thermal ALE process of metal can be constructed by combining the

two steps of oxidation and of etching of the oxidized layer by the formation of volatile organometallic complexes. In this ALE process, it is important that the etchant organic gas molecules do not form volatile organometallic complexes on the metallic surface so that the metal surface is not etched by the etchant gas. In this way, the etching of the oxidized layer stops when the metal surface is exposed to the etchant gas, which is termed a self-limiting step. In the ALE process, the cycle comprising the oxidation step and the self-limiting oxide etching step is repeated a predefined number of times so that the metal surface can be etched to a desired depth in a controlled manner.^{1,7,11}

The self-limited nature of the oxide etching step arises from the fact that hfacH is unstable and dissociates on an Ni surface, which has been confirmed experimentally.^{1,7} However, the mechanisms of

this stability, explaining the reasons why an hfacH molecule decomposes on an Ni surface while it forms $\text{Ni}(\text{hfac})_2$ on an NiO surface, have not been well understood prior to this study. As the first step to understand these phenomena, therefore, we examine herein the stability of hfacH molecules adsorbed on Ni and NiO surfaces using first-principles quantum mechanical (QM) simulations.

The goal of this study is to present qualitative insight into the mechanisms of the adsorption of hfacH on Ni and NiO surfaces. More specifically, our aim is to answer why an hfacH molecule tends to be adsorbed stably on an NiO surface, whereas it tends to decompose on an Ni surface. As mentioned above, the adsorption processes play a crucial role in establishing the self-limiting etching step of NiO by hfacH exposure at an elevated temperature. Although we use first-principles QM simulations to achieve this goal, a precise evaluation of the reaction energies for adsorption (i.e., adsorption energies) on a real Ni or NiO surface is beyond the scope of the present study. This is owing to the highly complex nature of the QM simulation for such systems. Therefore, as is shown in the subsequent sections, we employ simple models for the hfacH adsorption processes and analyze the model systems using QM simulation.

II. MODELING

The simulation of this study was performed with GAUSSIAN 09 Revision D.01¹² software. Our QM simulation is based on the density functional theory (DFT) with the B3LYP functional^{13–15} and the 6-311G(d) AO basis set.¹⁶ The QM simulation was used to evaluate the total energy of a system consisting of multiple atoms (e.g., a single molecule or a system of a molecule interacting with a surface) in its ground state, when the positions of all nuclei were fixed in space. The QM simulation was also used to obtain the most stable atomic configuration (geometric configuration) of a system at zero temperature. The latter is called geometry optimization. Partial geometry optimization can be performed with the positions of some selected atoms being fixed.

The accuracy of system energy evaluated by such a simulation depends on the assumptions used in the numerical techniques. In the DFT framework, the most suitable functionals need to be selected for quantitative evaluation of the system energy. However, it cannot be known *a priori* which functionals are the most suitable for the system one wants to calculate. It is generally believed that B3LYP offers reasonable computational results for organic systems as well as systems containing transition metals such as Ni.^{13–15} This is why we used B3LYP in our simulation presented in this study. However, there have been many studies comparing various functionals for DFT calculations,^{14,15,17–20} which typically show that the selection of best functionals depends on the system and the physical quantities (such as reaction energies, bond lengths, band structures, vibrational frequency shifts, etc.) to be evaluated. Discussion on the most appropriate selection of DFT functionals is beyond the scope of the present work and deferred to a future study.

Similarly, we used the 6-311G(d) basis set as it is widely used in DFT calculations in general.¹⁶ It should be noted, however, that the 6-311G(d) basis set does not include the diffuse functions, the use of which could improve the representation of highly polarized

atoms. Furthermore, we did not include the dispersion interaction (i.e., van der Waals interaction) in our simulation for the sake of simplicity. The dispersion interactions have much lower attractive interaction energies than those of typical covalent bond interactions but are of much longer range. In this study, we assume that the effects of dispersion interactions on adsorption energies are relatively minor and do not alter our conclusion on the adsorption mechanisms of hfacH on Ni and NiO surfaces. However, the inclusion of dispersion interactions is necessary for the quantitative evaluation of adsorption energies and barriers.

Owing to the high cost of QM simulations in general, it is practically impossible to employ, as a computational model system, a realistic system comprising an hfacH molecule incident upon a surface material that consists of a large number of atoms. Therefore, to represent the material surfaces, we used reduced models of single monolayers that can capture the essential nature of the real NiO and Ni surfaces. Figure 1 shows the top views of the (100) single-monolayer rectangular surfaces of fcc NiO ($8.89 \times 8.89 \text{ \AA}^2$) and Ni ($7.48 \times 4.98 \text{ \AA}^2$). In each case, the total net charge was assumed to be zero. In the geometry optimization of an hfacH adsorption process performed in this study, the positions of all surface atoms were fixed, while the geometric structure of an hfacH molecule was optimized. In the reality, as an adsorbate molecule approaches the surface, the positions of surface atoms interacting with the adsorbate can change. However, we assumed that such changes in the positions of surface atoms were sufficiently small. The geometry optimization was performed with gradient minimization techniques.

As mentioned earlier, the goal of this study is to present qualitative insight into the mechanisms of the adsorption of hfacH on Ni and NiO surfaces. As the first step, we looked at adsorption processes of an hfacH molecule with Ni and NiO simple single-layer surface models mentioned above. To simplify the simulation further, we have employed several approximations for DFT calculations, as discussed earlier. The validity of the surface models as well as the use of the approximations for DFT calculations must be validated eventually. However, our preliminary DFT calculations of the same adsorption processes with larger and more realistic surface models based on different DFT calculation methods including dispersion interactions have also shown that the results are qualitatively consistent with what is presented in this article. Therefore, we are confident that our simulation results presented in this article help us understand, at least qualitatively, the mechanisms on how an hfacH molecule interacts with an Ni or NiO surface. A systematic study of the accuracy of simulation results presented in this article is deferred to a future work.

III. RESULTS AND DISCUSSION

First, we optimized the structures of the keto and enol types of hfacH using our simulation, which are shown in Fig. 2. The enol-type hfacH is known to be more stable than the keto type. The energy difference obtained from our simulation is -27.48 kJ/mol (-0.285 eV), which is consistent with the results of earlier studies.^{21–25} This result implies that the majority of hfacH in the gas phase exists in the enol form and, therefore, in the simulations herein, we used only the enol-type hfacH as an adsorbate.

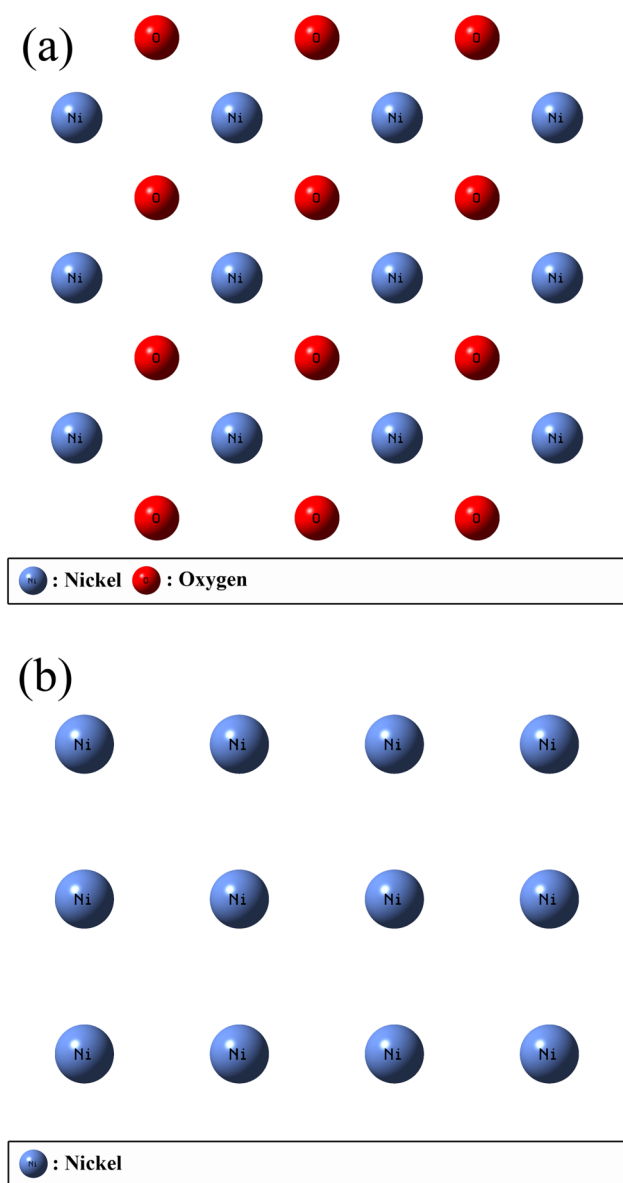


FIG. 1. Top views of the single-monolayer surface models used in the simulations. (a) $8.89 \times 8.89 \text{ \AA}^2$ square (100) surface of fcc NiO and (b) $7.48 \times 4.98 \text{ \AA}^2$ rectangular (100) surface of fcc Ni.

To obtain partial charge distributions, we used a natural bond orbital (NBO) population analysis. Figure 3 shows the NBO charge distributions of both types of hfach. Figure 3(a) shows that the oxygen atoms are the most negatively charged with a charge of $-0.448 e$ (with e being the elementary charge) in the keto type. Furthermore, Fig. 3(b) shows that the oxygen bonded with the hydrogen atom has a charge of $-0.615 e$, while the other oxygen atom has a charge of $-0.570 e$ for the enol type. It should be noted

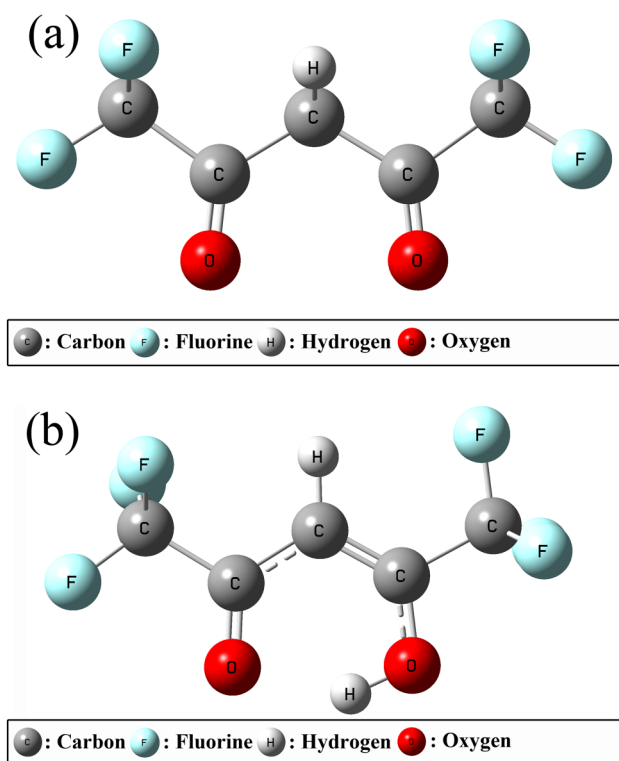


FIG. 2. Simulated optimized structures of (a) keto-type and (b) enol-type hfach molecules. The enol-type hfach is more stable than the keto-type, with an energy difference of -0.285 eV .

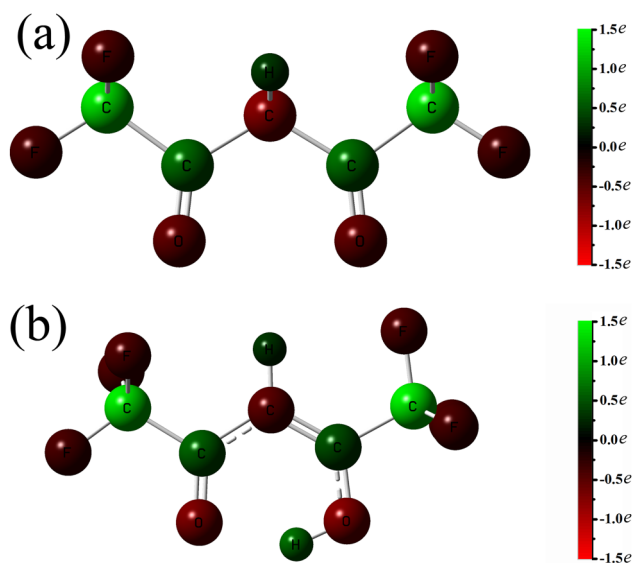


FIG. 3. NBO charge distribution from $-1.5 e$ (red color) to $1.5 e$ (green color) of (a) keto-type and (b) enol-type hfach molecules. It is seen that oxygen atoms are most negatively charged in each molecule.

that the fluorine atoms are negatively charged (-0.335 to $-0.356 e$), whereas the carbon atoms of trifluoromethyl ($-\text{CF}_3$) groups are highly positively charged ($+1.050$ to $+1.075 e$), which makes hfacH a highly polarized molecule.

We also examined the charge distributions of the model surfaces, as shown in Fig. 4. As expected, the simulation shows that NiO is an ionic crystal that consists of positively charged Ni and negatively charged O atoms. In contrast, the Ni atoms of the metallic Ni surface are nearly charge neutral.

Now, we examine how an hfacH molecule interacts with the model NiO surface of Fig. 4(a) when it approaches the surface. There are many possibilities for the orientation of an hfacH

molecule when it approaches a surface. In this study, we studied three different orientations of an hfacH molecule: (1) an hfacH molecule vertically aligned toward the NiO surface with the oxygen atoms closer to the surface, as shown in Fig. 5 (this atomic configuration was called “NiO + hfacH”); (2) an hfacH molecule vertically aligned toward the surface but in the opposite direction, with the F atoms being closer to the surface, as shown in Fig. 6 (“NiO + inv. hfacH”); and (3) an hfacH molecule tilted at an angle of 56° from the configuration, as shown in Fig. 7 (“NiO $\sim 56^\circ$ hfacH”). The tilting angle was measured from the surface normal, so that the vertical hfacH was defined as tilted at an angle of 0° . In all three

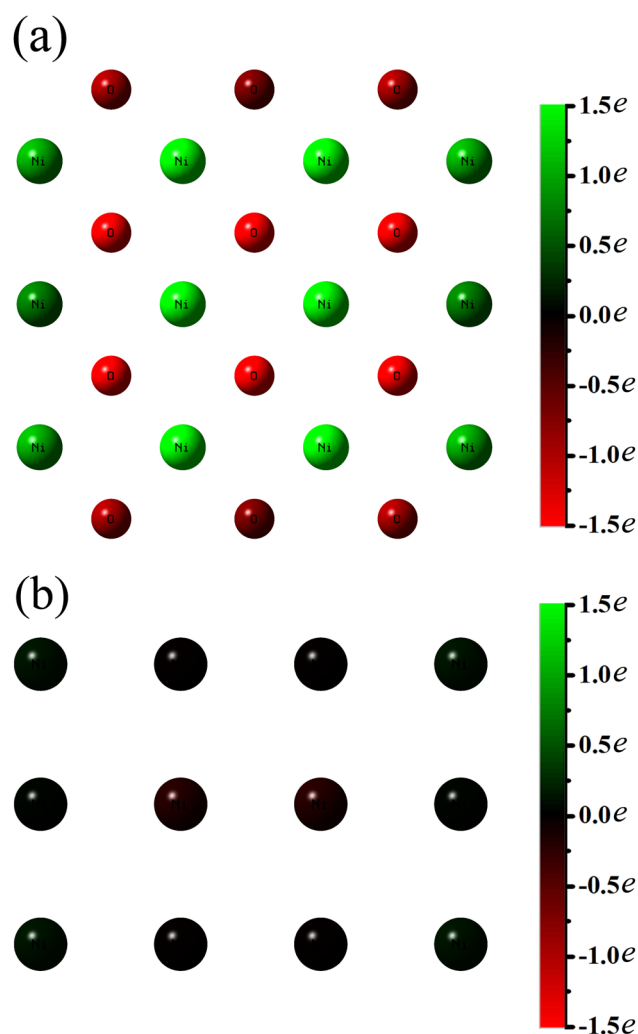


FIG. 4. NBO charge distribution from $-1.5 e$ (red color) to $1.5 e$ (green color) of model surfaces of (a) NiO and (b) Ni given in Fig. 1. It is seen that NiO is an ionic crystal that consists of positively charged Ni and negatively charged O atoms, whereas Ni of the metallic surface is nearly charge neutral.

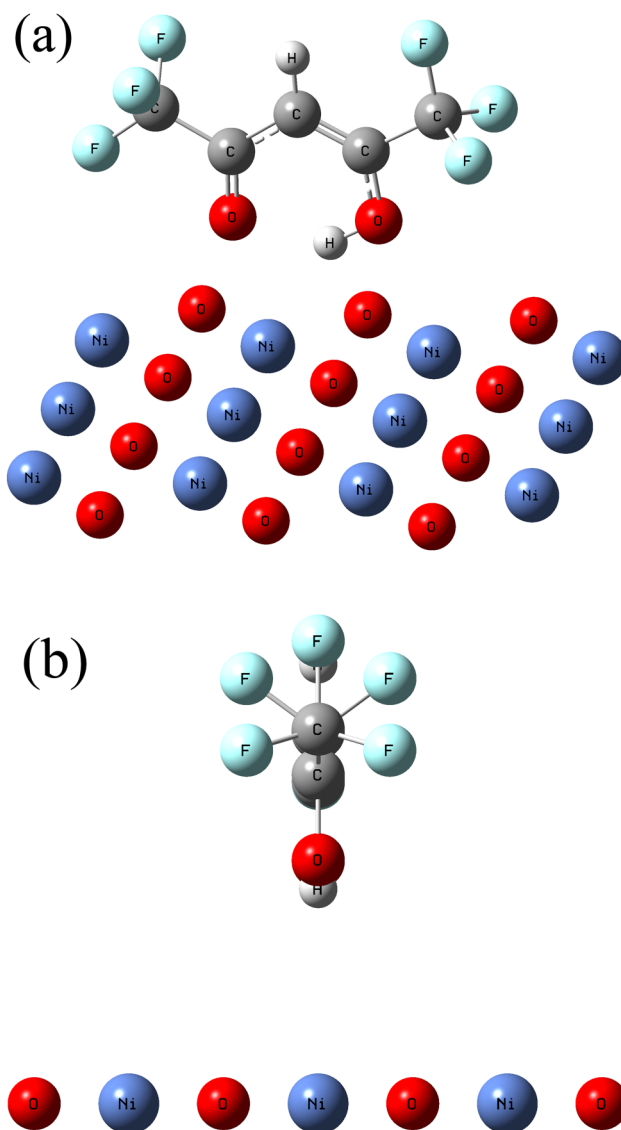


FIG. 5. “NiO + hfacH”, where an hfacH molecule is vertically placed on an NiO monolayer: (a) front view and (b) side view.

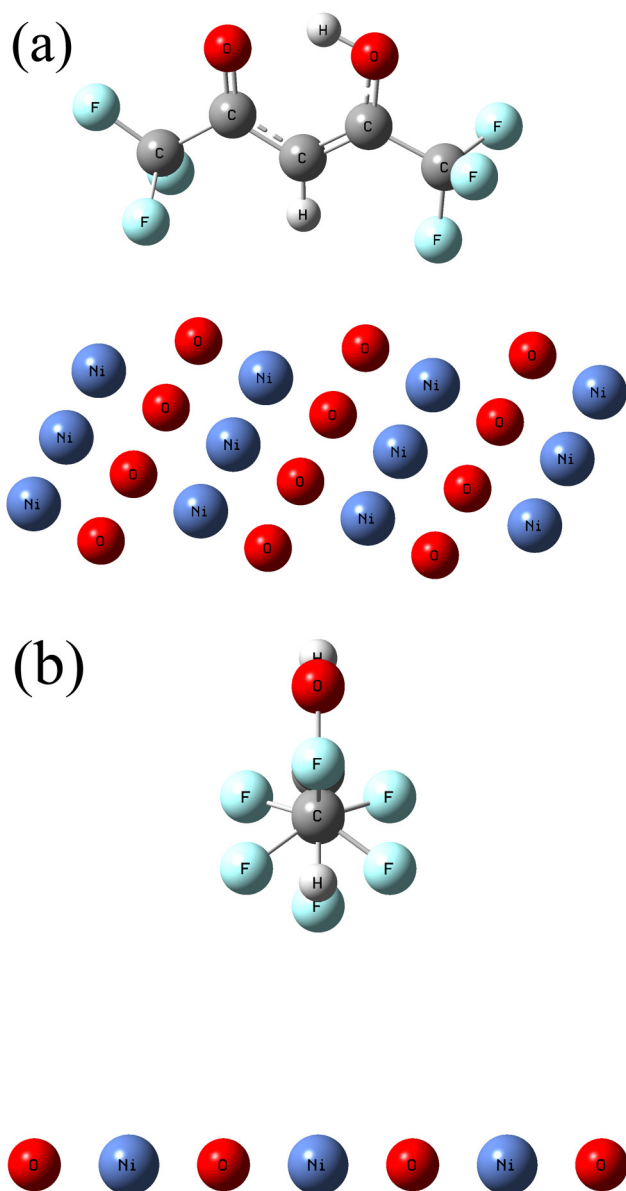


FIG. 6. “NiO + inv. hfach”, where an inverted hfach molecule is vertically placed on an NiO monolayer: (a) front view and (b) side view.

cases, each O atom of the hfach molecule was placed nearly above one of the two central Ni atoms of the surface with the same distance from the NiO surface plane.

In the simulation, we first evaluated the “interaction energy” between an hfach molecule of a fixed geometric configuration and the fixed model surface as a function of distance between the molecule and the surface. The distance between the hfach molecule and the surface was defined as the position of the O atoms of the hfach molecule measured from the NiO surface plane. In this

configuration, the two O atoms were placed in parallel to the NiO surface plane. The “interaction energy” was defined as

$$\text{Interaction energy} = E_t - E_1 - E_2, \quad (1)$$

where E_t is the total energy of the system, E_1 is the total energy of the hfach molecule, and E_2 is the total energy of the NiO model

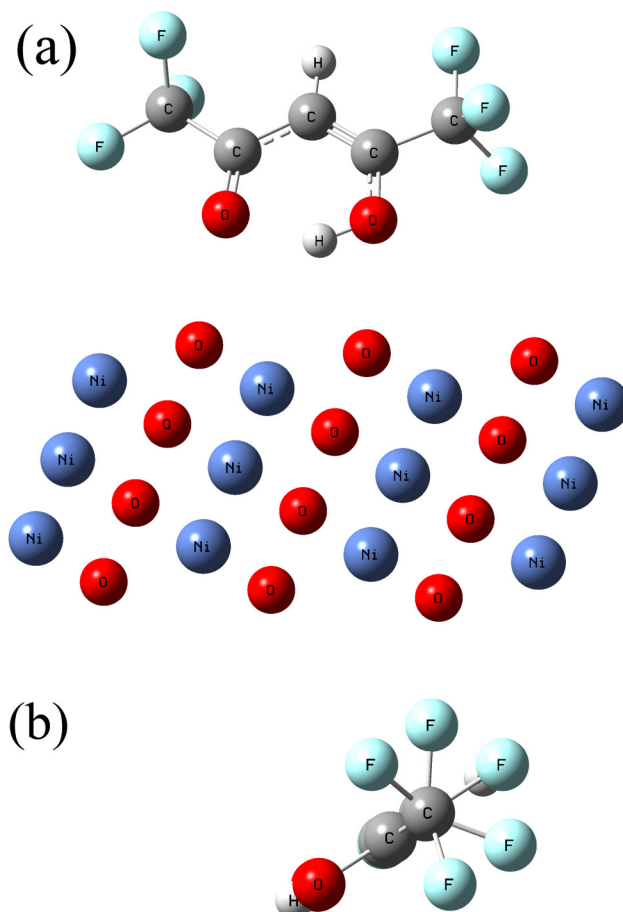


FIG. 7. “NiO ~ 56° hfach”, where an hfach is tilted at an angle of 56° on an NiO monolayer: (a) front view and (b) side view.

surface, all at zero temperature. Figure 8 gives the interaction energy from Eq. (1) for an hfacH molecule with an atomic configuration of Fig. 2(b) and an orientation of Figs. 5, 6, or 7, and the model (100) NiO surface of Fig. 4(a), as functions of the distance between the hfacH molecule and the surface. No geometry optimization was performed for this evaluation. In this sense, these calculation results only present a rough idea of how hfacH molecules in the three different orientations given in Figs. 5–7 interact with the NiO surface. Figure 8 suggests that the tilted hfacH molecule interacts with the NiO surface most stably with the lowest interaction energy among the three cases examined here.

Based on this observation, we placed a 56° tilted hfacH molecule at a distance of 2.6 \AA (i.e., the lowest-energy position in Fig. 8) above the NiO surface as the initial configuration and performed a geometry optimization. As mentioned earlier, all surface Ni and O atoms were assumed to be immobile but the positions of all atoms of the hfacH molecule were optimized. The atomic configuration of the minimum energy state of this system is shown in Fig. 9. It is seen that the hfacH molecule is deprotonated, with the hydrogen (H) atom between its two oxygen atoms transferred to one of the oxygen atoms of the NiO surface. As a result, the hexafluoroacetylacetonate anion (hfac $^-$) is bonded with the NiO surface with an interaction of the two O atoms of hfac $^-$ with two adjacent Ni atoms of the NiO surface. At least qualitatively, the simulation result here showing that an hfacH molecule is adsorbed stably (in the form of an hfac $^-$ anion) on an NiO surface is consistent with the experimental observations of Refs. 1 and 7.

The interaction energy, as defined in Eq. (1) with the optimization of E_t with fixed positions of all NiO model surface atoms [whose atomic configuration is given in Fig. 9], is -2.02 eV , with

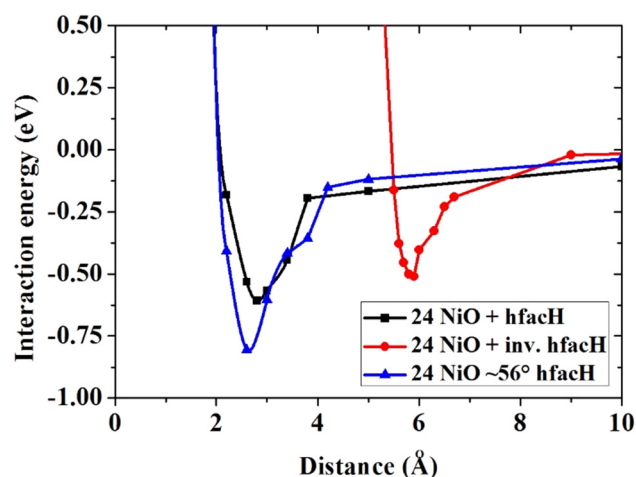


FIG. 8. Interaction energies between the NiO surface and hfacH molecules with the three different orientations given in Figs. 5–7 as a function of the distance between the surface and the hfacH molecule, defined as the position of the O atoms of the hfacH molecule measured from the NiO surface plane. It should be noted that no geometry optimization is performed in this simulation so that the atomic configuration of an hfacH atoms is the same as that of Fig. 2(b) (of enol type) and the surface model is given by Fig. 4(a). The curves and lines are guides for the eye.

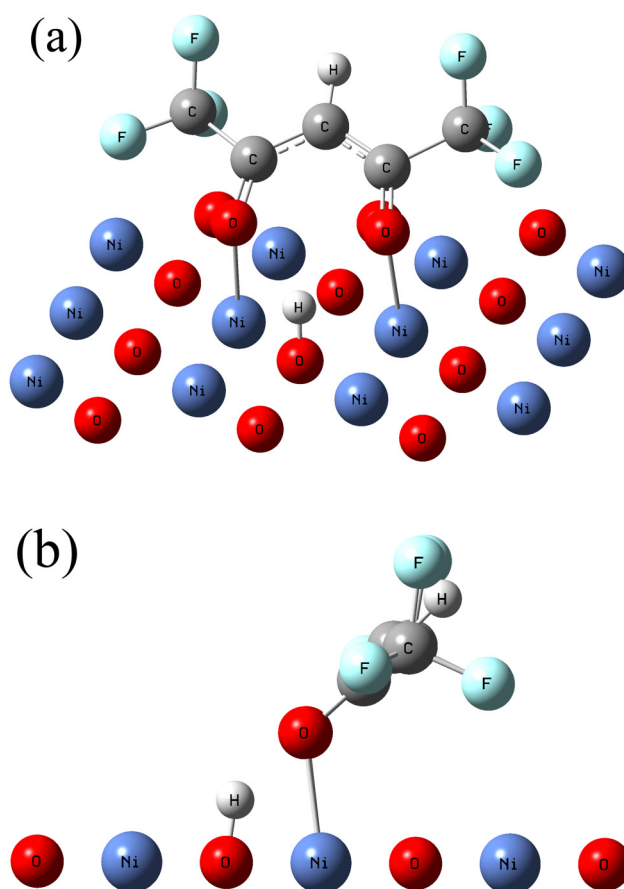


FIG. 9. Optimized structure²⁶ of an hfacH adsorbed on the NiO model surface: (a) front view and (b) side view. It is seen that, after structural optimization of hfacH (with a fixed NiO structure), hfacH is deprotonated and hfac $^-$ is stably bonded with the surface.

the zero-point corrected total energy.¹² This is the adsorption energy, or the “reaction energy,” of an hfacH molecule’s adsorption on the NiO surface for the model system. The bond length between an O atom of hfac $^-$ and its closest Ni atom of the NiO surface is about 2.05 \AA and the hfac $^-$ is tilted with an angle of about 46° against the surface normal. The adsorption energy and the bond length obtained in this study are similar to those reported on the adsorption of hfacH on a ZnO surface by Kung and Teplyakov.²⁵ It should be noted, however, the adsorption energy, bond length, and tilting angle given above are obtained from our DFT calculations of simplified models and should not be construed as the exact values of the real system, as we cautioned in Sec. II.

The electrical charge distribution (NBO population) of the system of Fig. 9 is shown in Fig. 10. The NBO charge distribution of the H atom on the NiO surface is $0.844 e$ and the total charge of hfac $^-$ shown in Fig. 10 is $-0.844 e$. The simulation result suggests that the deprotonation of an hfacH molecule occurs because of the presence of negatively charged O atoms on the surface. In addition, it is clearly seen that the negatively charged O atoms of hfac $^-$ are

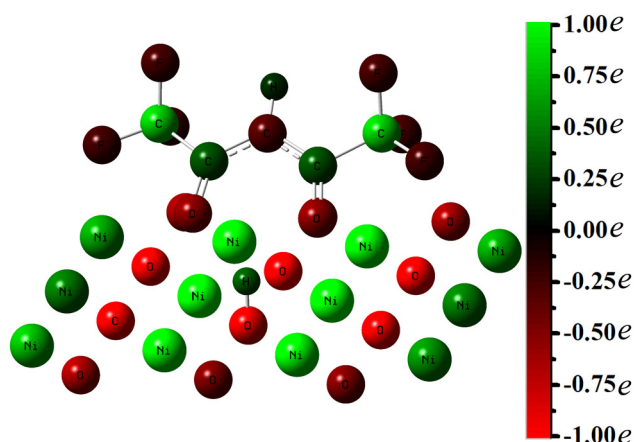


FIG. 10. NBO charge distribution from $-1.0\ e$ (red color) to $1.0\ e$ (green color) of the system given in Fig. 9.

bonded with positively charged Ni atoms. In other words, the presence of ionic bonds; i.e., the fact that Ni atoms are positively charged and O atoms are negatively charged in the NiO surface; is the main reason for the deprotonation and stable adsorption of an hfacH molecule. A similar mechanism should also function for the adsorption of polarized molecules such as diketones on a surface with ionic bonds, such as an oxidized or halogenated metal surface.

We now discuss hfacH adsorption on a metallic Ni surface. It is known that hfacH molecules are dissociated when they approach a metallic Ni surface at room temperature or higher, which has been observed experimentally.^{1,7} Figure 11 shows the optimized structure of an hfacH molecule placed at the center of the $7.48 \times 4.98\ \text{\AA}^2$ Ni monolayer surface given in Fig. 1(b). The molecule was initially placed at a distance of $2.2\ \text{\AA}$ above the surface plane with a tilt angle of 56° , in a fashion similar to Fig. 9. As before, the distance was defined as the position of the O atoms of the hfacH molecule measured from the surface plane. The two O atoms were originally placed above the two Ni atoms near the center of the rectangular Ni monolayer surface. It is seen in Fig. 11 that, after a geometry optimization (with the positions of all Ni atoms being fixed), the hfacH molecule moved closer to the Ni surface and was decomposed without deprotonation. Dissociated F atoms went to the opposite side of the monolayer surface, which of course may not occur in an actual Ni surface. The reaction energy for the atomic configurations given in Fig. 11 is $-8.70\ \text{eV}$, with the zero-point corrected total energy.¹² This large absolute value of the reaction energy arises from the formation of Ni—F and Ni—C bonds after some F atoms are removed from the hfacH molecule. On a metallic Ni surface, such reaction energy varies depending on how the adsorbed hfacH molecule is decomposed on the surface.

The NBO charge distribution of the system of Fig. 11 is shown in Fig. 12. It is seen that Ni atoms of the surface are nearly charge neutral except for those interacting closely with the F and C atoms. The simulation result suggests that, in the case of a metal surface, the negatively charged O atoms and the positively charged H atom between them in an hfacH molecule have no particular surface atoms

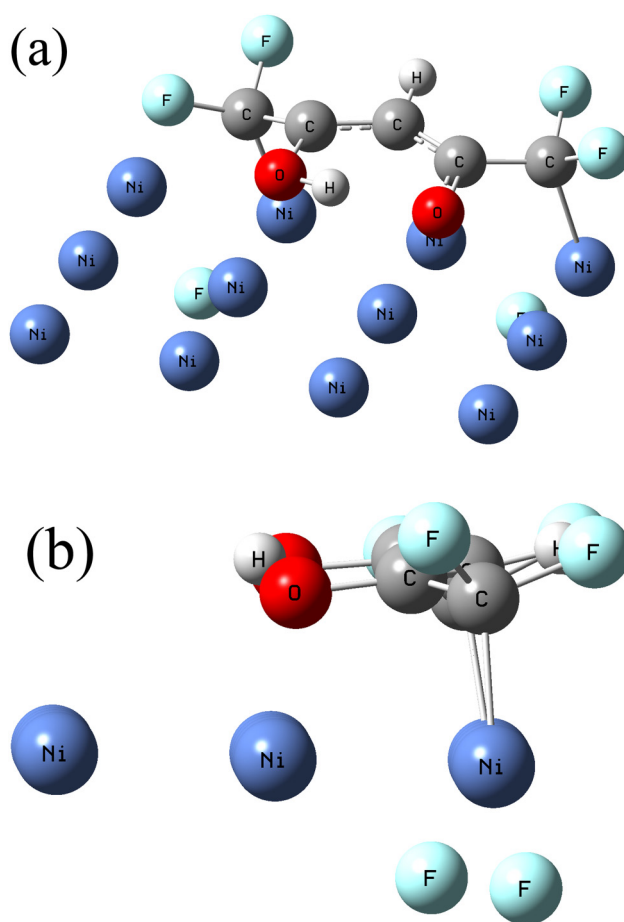


FIG. 11. Optimized structure²⁶ of an hfacH molecule placed near a metallic Ni model surface given in Fig. 1(b); (a) front view and (b) side view.

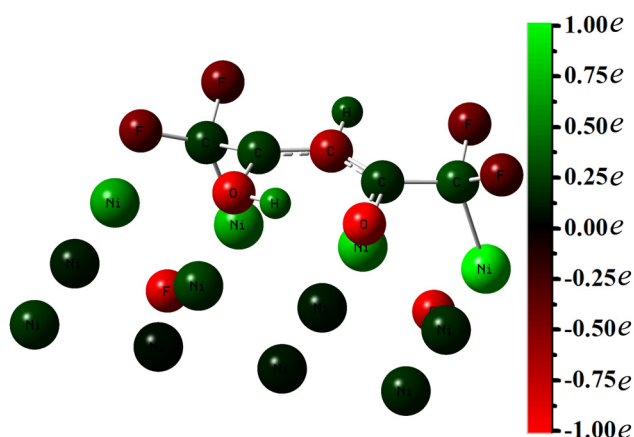


FIG. 12. NBO charge distribution from $-1.0\ e$ (red color) to $1.0\ e$ (green color) of the system given in Fig. 11.

with which to bond because all surface metal atoms are charge neutral. Therefore, deprotonation of hfacH is unlikely to occur and, if the hfacH molecule is tilted down further, some of its F and C atoms can form bonds with Ni atoms on the surface, as seen in Fig. 11.

IV. SUMMARY AND CONCLUSIONS

In this study, DFT-based first-principles QM simulations were used to clarify why hfacH can be adsorbed stably on an NiO surface while it can be dissociated on a metallic Ni surface. The simulation results showed that, when a stable enol hfacH molecule approaches an NiO surface, its negatively charged O atoms are attracted to Ni atoms of the NiO surface, where all Ni atoms are positively charged. If the distance between the hfacH molecule and the NiO surface is sufficiently short, the system becomes more stable once the H atom located between the two O atoms of hfacH is transferred to a nearby surface O atom. In this process, the dissociated H atom is positively charged and the remaining part, i.e., hfac[−], is negatively charged (i.e., deprotonation of hfacH). Because of this charge transfer, the two negatively charged O atoms of hfac[−] are bonded more strongly with positively charged surface Ni atoms. Once this structure is established, the adsorbed hfac[−] anion may be slightly tilted but will not fall down on the NiO surface. This prevents the strong interaction of its C and F atoms with surface atoms and the breakdown of the hfac[−] anion on the surface, as our simulation indicates. In this sense, the adsorption of hfac[−] anion on an NiO surface is stable.

Conversely, on an Ni metallic surface, every Ni surface is equally charged or charge neutral if the surface is charge neutral. Therefore, when an hfacH molecule approaches a metallic Ni surface, there are no particular preferential sites to which it can stably attach and it is less likely to transfer its H atom or H⁺ cation to the surface (i.e., to deprotonate). At room temperature or higher, accidental tilting of an hfacH molecule allows its C and F atoms to be bonded with surface Ni atoms, resulting in the dissociation of hfacH on a metallic surface.

These results are qualitatively consistent with experimental observations obtained in earlier studies.^{1,5,7} The results of this work indicate that the adsorption of hfacH or other diketones (or even other polarized molecules) on a surface is promoted by the presence of ionic bonds (or polarization) on the surface. On an oxidized or halogenated metal surface, surface atoms are polarized, and approaching diketones may similarly deprotonate and have their O atoms bonded with positively charged metal atoms on the surface. On a metal surface, however, such polarized molecules cannot find any preferred adsorption sites and may disintegrate when they approach the surface closely.

As discussed earlier, small surface models were employed herein to represent Ni and NiO surface for analysis via first-principles QM simulations. Furthermore, we have not yet tested various DFT functionals with dispersion interactions or basis sets with the diffuse functions. Therefore, the values of adsorption energies and other physical quantities obtained in this study should not be construed to represent the true values of a real system, where the surface size is far greater than the hfacH molecule. More accurate evaluation of the reaction energies via DFT-based first-principles QM simulations for larger systems is a subject of a future study.

Stable adsorption of hfacH is only the first step of the thermal ALE process of a metal surface. At an elevated surface temperature,

adsorbed hfac[−] anions on a metal oxide surface form volatile organometallic complexes such as Ni(hfac)₂. Analysis of the formation process of such organometallic complexes is also beyond the scope of the present study and is deferred to a future work.

ACKNOWLEDGMENTS

A.H.B. appreciates support from Professional Development Consortium for Computational Materials Scientists (PCoMS), which allowed him to visit M.K. and W.W. at KIT, Germany, during this study. A.H.B. and S.H. are also grateful to Yoshitada Morikawa and Ikutaro Hamada of Osaka University for fruitful discussion. This work is partially supported by the Japan Society of the Promotion of Science (JSPS) Grants-in-Aid for Scientific Research (S) (No. 15H05736), JSPS Core-to-Core Program, and by Deutsche Forschungsgemeinschaft (DFG, German Research Foundation) under Germany's Excellence Strategy—2082/1-390761711 and GRK 2450.

REFERENCES

- H. L. Nigg and R. I. Masel, *J. Vac. Sci. Technol. A* **17**, 3477 (1999).
- G. O. Hunter and B. D. Leskiw, *Rapid Commun. Mass Spectrom.* **26**, 369 (2012).
- Y. Duan, F. Gao, and A. V. Teplyakov, *J. Phys. Chem. C* **119**, 27018 (2015).
- S. M. George and Y. Lee, *ACS Nano* **10**, 4889 (2016).
- J. K. Chen, T. Kim, N. D. Altieri, E. Chen, and J. P. Chang, *J. Vac. Sci. Technol. A* **35**, 031304 (2017).
- J. K. Chen, N. D. Altieri, T. Kim, E. Chen, T. Lill, M. Shen, and J. P. Chang, *J. Vac. Sci. Technol. A* **35**, 05C305 (2017).
- T. Ito, K. Karahashi, and S. Hamaguchi, in *Proceedings of the 39th International Symposium on Dry Process*, Tokyo, Japan, 16–17 November 2017, edited by K. Kinoshita et al. (DPS Organizing Committee, 2017), Vol. E-4, p. 45.
- K. J. Kanarik, S. Tan, and R. A. Gottscho, *J. Phys. Chem. Lett.* **9**, 4814 (2018).
- J. Zhao, M. Konh, and A. V. Teplyakov, *Appl. Surf. Sci.* **455**, 438 (2018).
- M. Konh, C. He, X. Lin, X. Guo, V. Pallem, R. Opila, A. Teplyakov, Z. Wang, and B. Yuan, *J. Vac. Sci. Technol. A* **37**, 021004 (2019).
- S. Kang, H. Kim, and S. Rhee, *J. Vac. Sci. Technol. B* **17**, 154 (1999).
- M. J. Frisch et al., *Gaussian 09*, Revision D.01 (Gaussian, Inc., Wallingford, CT, 2013).
- S. Grimme, *J. Chem. Phys.* **124**, 034108 (2006).
- M. Steinmetz and S. Grimme, *ChemistryOpen* **2**, 115 (2013).
- S. Paranthaman, S. Sampathkumar, and N. K. Murugasenapathi, *J. Chem. Sci.* **130**, 164 (2018).
- R. Krishnan, J. S. Binkley, R. Seeger, and J. A. Pople, *J. Chem. Phys.* **72**, 650 (1980).
- M. C. Holthausen, *J. Comp. Chem.* **26**, 1505 (2005).
- R. Valero, J. R. B. Gomes, D. G. Truhlar, and F. Illas, *J. Chem. Phys.* **132**, 104701 (2010).
- X. Xu and D. G. Truhlar, *J. Chem. Theory Comput.* **8**, 80 (2012).
- Y. Sert, F. Uzun, G. A. El-Hiti, K. Smith, and A. S. Hegazy, *J. Spectrosc.* **2016**, 5396439 (2016).
- M. da Silva, L. Santos, and E. Giera, *J. Chem. Thermodyn.* **39**, 361 (2007).
- K. Manbeck, N. Boaz, N. Bair, A. Sanders, and A. Marsh, *J. Chem. Educ.* **88**, 1444 (2011).
- S. Engmann, B. Ómarsson, M. Lacko, M. Stano, Š Matejčík, and O. Ingólfsson, *J. Chem. Phys.* **138**, 234309 (2013).
- D. L. Howard, H. G. Kjaergaard, J. Huang, and M. Meuwly, *J. Phys. Chem. A* **119**, 7980 (2015).
- H. Kung and A. Teplyakov, *J. Catal.* **330**, 145 (2015).
- See supplementary material at <https://doi.org/10.1116/1.5127532> for the Cartesian coordinates of the optimized structures of Figs. 9 and 11.